

RESEARCH ARTICLE



OPEN ACCESS

Received: 10-05-2024

Accepted: 17-06-2024

Published: 28-06-2024

Citation: Bhavsar J, Patel A, Patel K (2024) Improved Sparse Representation of Image from Inferred Angles of Steerable Wavelet. Indian Journal of Science and Technology 17(26): 2698-2707. <https://doi.org/10.17485/IJST/v17i26.1385>

* **Corresponding author.**

jignesh@gecg28.ac.in

Funding: None

Competing Interests: None

Copyright: © 2024 Bhavsar et al. This is an open access article distributed under the terms of the [Creative Commons Attribution License](#), which permits unrestricted use, distribution, and reproduction in any medium, provided the original author and source are credited.

Published By Indian Society for Education and Environment ([iSee](#))

ISSN

Print: 0974-6846

Electronic: 0974-5645

Improved Sparse Representation of Image from Inferred Angles of Steerable Wavelet

Jignesh Bhavsar^{1*}, Amrutbhai Patel², Kalpesh Patel¹

¹ Assistant Professor, Electronics and Communication Department, Government Engineering College, Sector 28, Gandhinagar, Gujarat, India

² Associate Professor, Electronics and Communication Department, Ganpat University- U.V.Patel College of Engineering, Mehsana, Gujarat, India

Abstract

Objectives: Presenting images with sparse coefficients has a wide variety of real-time applications in compressive sensing. However, sparse representations of images present challenges due to hidden similarities in the higher order moments. Literature suggests that the applications that involve natural images present a high level of similarity. Steerable basis, due to their rotational invariant property, have shown potential in sparse representation of natural images. Hence, the objective of the proposed study is to identify steerable basis that maximize the sparse representation of natural images. **Method:** Prior studies have used the angle of steerable basis either from the random assignment or derived from Hough transform. In this study, we propose the selection of steerable basis angle derived from maximum a prior method. Exploiting a steerable basis for better sparse representation requires the knowledge of proper steerable angles. Hence, we propose using MAP learning approach to identify this angle. **Findings:** The proposed method resulted in optimal steerable angle without the need for calculation of Hough Transform. In addition, the method also resulted in almost 10 percent improvement in sparse representation as indicated by higher Kurtosis. **Novelty:** We compare the measure of sparsity to evaluate the effectiveness of the proposed method. The results indicate the optimal sparsity from the proposed method as indicated from the maximum values of kurtosis compared to the previous related methods. In addition, the proposed method relaxes the requirement of manipulating Hough transform for optimal steerable angle.

Keywords: Sparsity; Steerable Basis; Wavelet Pyramid Structure; Image Compression; Hough Transform

1 Introduction

An image characterized by sparsity exhibits substantial information content in a limited set of coefficients. The motivation for seeking sparse representations of images is rooted in the fact that a sparse image representation enables more efficient compression. This is due to the reduced number of coefficients required to represent the image. Furthermore,

sparse representations offer benefits beyond compression, extending their applicability to various domains. For example, sparse transformation of signal permits to little violate Nyquist sampling theorem without loss of fidelity⁽¹⁾, computationally efficient computer vision and object recognition algorithms⁽²⁾, improved speech processing, financial time-series analysis, and communications⁽³⁾. Sparse representation can be used to recover poor sampled image⁽⁴⁾.

To obtain sparse coefficients, it is essential to choose a suitable basis that captures the underlying structure of the image. In the context of image processing, sparse representations can be achieved through various techniques, such as the Discrete Cosine Transform (DCT) and Wavelet Transform. These techniques can be used to represent images sparsely enabling efficient processing and analysis. For instance, in object recognition, sparse transformations can be used to extract features from images, leading to improved classification performance and efficiency⁽²⁾. Discrete Cosine Transform, Wavelet Transform and other sparse representation can also be used for different applications like classification⁽⁵⁾, face recognition⁽⁶⁾, image denoising⁽⁷⁾ and image fusion⁽⁸⁾. This transformation compromises the compression efficiency while working with natural images. Natural images have dominant number of edges in particular directions, making these transformations with static structures-less convergent to optimal compression efficient⁽⁹⁾. This has led to the development of transformation with steerable basis which can be tuned to the direction of dominant edges. This captures maximum variations of the image with the least number of nonzero coefficients⁽¹⁰⁾⁽¹¹⁾.

Due to these limitations past research has investigated how to obtain/select suitable sparse basis. In⁽¹²⁾ machine learning-based techniques is investigated for finding suitable sparse basis coefficients⁽¹²⁾. These techniques aim to learn the distribution of coefficients, often with a sparse Cauchy prior, and adapt the basis to the signal using maximum a posteriori (MAP) estimation with minimum residual error as a constraint⁽¹²⁾. To get sparse coefficients, one needs to choose a suitable basis of transformation by means of learning. Another technique proposed in⁽¹³⁾ to get sparse coefficients belonging to transformation with Wavelet Pyramid Structure having steerable basis. Here authors used clue inferred from Hough transform to tune steerable basis and got comparable sparsity of belonging coefficients. Our observation for above mentioned technique is, learned real random basis which provides sparse transformation are direction-oriented band pass filter. By taking clue of above observation, we propose a novel method of angle learning of band pass filter which provide better sparse representation, in addition, without the need for calculation of Hough Transform. The systematic selection of angle for steer basis not only improves the sparse representation, it also provides the way to benchmark the process of sparse representation when represented using wavelet pyramid structure with steerable basis. Section 2 provides the mathematical background of the steerable wavelet pyramid structure. Two existed methods, one is learning based basis and, second is steer the angle of steerable basis by taking clue from Hough transform for given pyramid structure are discussed in Section 3. In Section 4, authors propose a new approach of learning of steerable basis with zero initial angle. The comparative results indicate maximum a prior learning-based selection of steerable basis does not require manipulation of Hough Transformation at the same time it also results in better compression efficiency as observed from high kurtosis of image coefficients.

1.1 Wavelet Pyramid Structure:

Wavelet pyramid structure composed of low pass, high pass and recursive steerable bandpass filters. The coefficients of these filters in this pyramid structure can be adjusted to ensure reconstruction of input image. Due to this, it has been used for image compression without loss of information. General equation for pyramid structure is given by⁽¹²⁾,

$$\hat{X}(\vec{w}) = \frac{\{|H_0(\vec{w})|^2 + |L_0(\vec{w})|^2(|L_1(\vec{w})|^2 + \sum_0^n |B_k(\vec{w})|^2)\}}{X(\vec{w}) + \text{aliasing terms}}$$

where, \hat{X} is the filtered image, x is an input image to the wavelet pyramid structure, H_0 is high-pass filter, L_0 is further decomposed into low pass and band pass components L_1 and B_i 's as shown in Figure 1. This decomposition is performed recursively using standard 2 by 2 decimation process as explained in⁽¹²⁾.

The decomposition as mentioned above result in reconstruction if the filters obey below mentioned constraints. The constraints are as follows⁽¹²⁾

1) Unitary Response,

$$|H_0(\vec{w})|^2 + |L_0(\vec{w})|^2(|L_1(\vec{w})|^2 + \sum_0^n |B_k(\vec{w})|^2) = 1$$

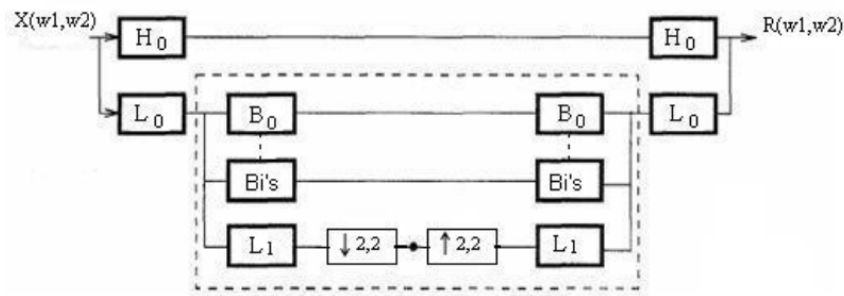


Fig 1. Pyramid structure of filters used for image decomposition

2) Recursion Relationship,

$$|L_1(\vec{w}/2)|^2 = (|L_1(\vec{w})|^2 + \sum_0^n |B_k(\vec{w})|^2) |L_1(\vec{w}/2)|^2$$

3) Aliasing Cancellation,

$$|L_1(\vec{w})| = 0 \text{ for } |\vec{w}| > \pi/2$$

In addition to above, B_i^s must satisfy following constraint,

$$B_k(\vec{w}) = B(\vec{w})[-j\cos(\theta - \theta_k)]^n,$$

$$\text{where } \theta = \arg(\vec{w}), \theta_k = \frac{\pi k}{(n+1)} \text{ for } k \in \{0, 1, \dots\}.$$

$$B(\vec{w}) = \sqrt{\sum_{k=0}^n |B_k(\vec{w})|^2}$$

Here Bi's are band pass filters representing the directional derivatives in θ_k direction. These are the oriented steerable basis as explained in 3.2.

Figure 2 shows the frequency spectrum of high pass, low pass and band pass filters. As evidenced from the frequency spectrum of bandpass filters (B0-B3), they are directionally oriented. The direction of these filters affects the compression efficiency. One way to select proper direction for better compression is to derive the angle of these bandpass filters from Hough Transformation⁽¹³⁾. However, each image requires calculation of Hough Transformation separately which makes its application to the limited use cases. To overcome this limitation, maximum a prior learning is suggested to derive the optimal direction of bandpass filter coefficients.

1.2 Steerable basis:

Definition: Steerable basis belongs to the bandpass filters of wavelet pyramid structure. Due to the unique property of rotational invariant, the bandpass filters can be steered to any direction in two-dimensional space⁽¹⁴⁾. Hence, these filters possess the capability of rotation through the application of a specific linear combination of a limited set of filters⁽¹⁵⁾. The M^{th} order two-dimensional steerable filter with position vector $x=(x,y)$, denoted as $h(x; y)$ or simply $h(x)$, can be defined as:

$$h(x) = h(x, 7) = \sum_{k=1}^M \sum_{i=0}^k \alpha_{k,i} \frac{\partial^{k-i}}{\partial x^{k-i}} \frac{\partial^i}{\partial y^i} g(x, y)$$

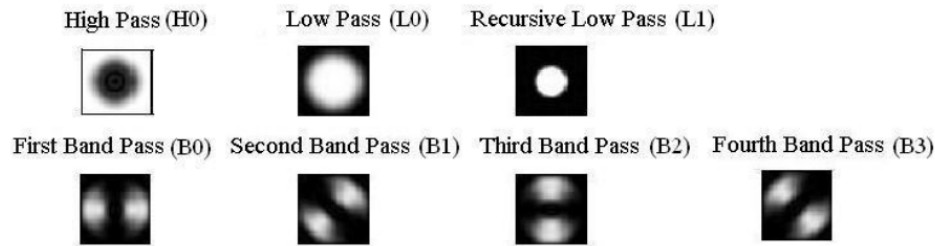


Fig 2. Spectra of Wavelet Pyramid Structure Family. H0 and L0 are respectively high pass and low pass filter used in Level-1, L1 and Bi's are used in recursion from the second level onwards

where $g(x, y)$ is any isotropic window function defined for image $f(x, y) = f(x)$, α_s are the coefficients of linear differential equation. The convolution of a $f(x, y)$ with any rotated variant of $h(x, y)$ is given by⁽⁹⁾,

$$f(x) * h(R_\theta x) = \sum_{k=1}^M \sum_{i=0}^k b_{k,i}(\theta) f_{k,i}(x)$$

Here,

$$f_{k,i}(x, y) = f(x, y) * \left(\frac{\partial^{k-i}}{\partial x^{k-i}} \frac{\partial^i}{\partial y^i} g(x, y) \right)$$

$$g_{k,i}(x, y)$$

$$R_\theta = \begin{bmatrix} \cos(\theta) & \sin(\theta) \\ -\sin(\theta) & \cos(\theta) \end{bmatrix}$$

$b_{\{k,i\}}(\theta)$ is interpolating coefficient⁽⁹⁾.

1.3 Inference from Hough Transform

In natural images, the presence of oriented lines and edges, particularly curved and fractal-like ones, causes higher-order statistical dependencies extending beyond simple pairwise correlations. This rationale supports the adoption of a Cauchy prior assumption. Within this framework, the coefficients of an image are optimized by maximizing the maximum a posteriori (MAP estimate). Learning aims to adjust the basis of the wavelet model to minimize the description length (L) of the images under the model. Consequently, the energy of the L2 signal remains finite and consistent before and after the transformation, indicating reliable signal reconstruction from the coefficients.

When steerable basis are finely tuned such that one basis aligns precisely perpendicular to the dominant direction of the edges, it captures most of the energy, leaving notably less energy for other directional steerable basis. As a result, coefficients associated with other directional basis tend toward zero, leading to an overall sparse distribution of coefficients. This mechanism does not necessitate explicit learning; instead, the direction with the highest energy is derived from the Hough space. However, we propose a learning-based approach to identify the direction of major energy preservation.

2 Methodology

We randomly selected natural images from the publicly available dataset⁽⁹⁾. This dataset consists of images captured from forest area where each image contains natural objects such as trees. Next, we discussed the proposed maximum a prior learning method to find optimal angle of steerable basis. With this method, we aim to adjust the coefficient of transformation with constraints to minimize error between actual image. At the same time, the learning should ensure the coefficient of image to follow Cauchy distribution so compress representation. The detailed explanation of the learning-based sparsity can be found in⁽¹²⁾. Images represent a linear combination of basis functions. By selecting specific basis coefficients, a, one can represent an

image $I(\vec{x})$ under the assumption of Gaussian, white, and additive noise.

$$I(\vec{x}) = \sum_i a_i \phi_i(\vec{x}) + v(\vec{x})$$

Here (\vec{x}) denotes a discrete spatial position, $\vec{\phi}_i$ represents basis functions, and v represents uncertainty or noise. Thus, for a given set of a_i 's, it is essential to find $\vec{\phi}_i$ so as to minimize of the noise. The ϕ_i 's are learned from the model based on the available data. The image I , as described in Equation (1), represented as:

$$I = Ga + \nu \quad (1)$$

In this equation, the vector a represents coefficients across all scales, positions, and levels, and G denotes the basis functions for the coefficient vector a . The probability of generating Image I , given coefficients a and assuming Gaussian i.i.d noise, is:

$$P(I/a, \theta) = \frac{1}{Z_{\lambda_N}} e^{-\frac{\lambda_N}{2} |I - Ga|^2}$$

Where θ is system parameters like scaling of Wavelet functions, noise variance is $1/\lambda_N$. Prior distribution of coefficient a is assumed to be sparse and factorized. Hence,

$$P(a) = \prod P(a_i)$$

and

$$P(a_i) = \frac{1}{Z_s} e^{-s(a_i)}$$

Where

$$s(x) = \beta \log(1 + (x/\sigma)^2)$$

is Cauchy like prior

In natural images, the presence of oriented lines and edges, particularly curved and fractal-like edges, leads to statistical dependencies that extend beyond linear pairwise correlations. This rationale justifies the adoption of a Cauchy prior assumption. Within this framework, the coefficients of a given image are determined by seeking the maximum a posteriori distribution (MAP estimate). The objective of learning is to learn the basis of the wavelet model in a manner that minimizes the description length L of images under the model.

$$\begin{aligned} \hat{a} &= \underset{a}{\operatorname{argmax}} P(I/a, \theta) \\ &= \underset{a}{\operatorname{argmax}} P(I/a, \theta) P(a/\theta) \\ &= \underset{a}{\operatorname{argmin}} \left[\frac{\lambda_N}{2} |I - Ga|^2 + \sum_i s(a_i) \right] \end{aligned}$$

Local minima found by gradient decent,

$$\dot{a} \propto \lambda_N G^T e - s(a)$$

$e = I - Ga$

Goal of learning is to adapt the basis of wavelet model that minimize description length L of images under the model,

$$L = -\log P(I/\theta)$$

$$P(I/\theta) = \int P(I/a, \theta) P(a/\theta) da$$

A learning rule basis functions may be derived by gradient descent on L,

$$\begin{aligned} \Delta \theta_i &= -\frac{\partial L}{\partial \theta_i} \\ &= \lambda_N \left\langle e^T \frac{\partial G}{\partial \theta_i} a \right\rangle_{P(a/I), \theta} \end{aligned}$$

3 Results and Discussion

The bandpass filters within the wavelet pyramid structures offer the advantage of steerable basis. That is, the adjustment of kernel of bandpass filter is determining factor how effective is the sparse representation for a particular image. Kurtosis is a direct measure for quantitative evaluation of sparsity. The kurtosis of filtered image coefficients should be higher for better sparsity. The adjustment in bandpass filter kernel affects the kurtosis of image coefficients. It is well-established in the literature that the kernel of BPF approaches a steerable basis when sparsity in the image coefficients increases, particularly for the case of natural images⁽¹²⁾. Additionally, the angle of steerable basis is also an important factor that determines the optimal compression. For instance, the image with many lines in vertical orientation and a few lines with other orientation will have the steerable basis more aligned in the vertical direction. The change in the direction of steerable basis changes kurtosis of image coefficients. Table 1 shows the values of kurtosis when the angle of steerable basis is varied. We observed that the selection of angle drastically affects kurtosis of image coefficients. For instance, kurtosis for an angle of 0 radian is 10.5524 whereas kurtosis for an angle of $-\pi/8$ radian is 9.8996. We found a change of almost 6.59 percent in kurtosis when the angle is changes.

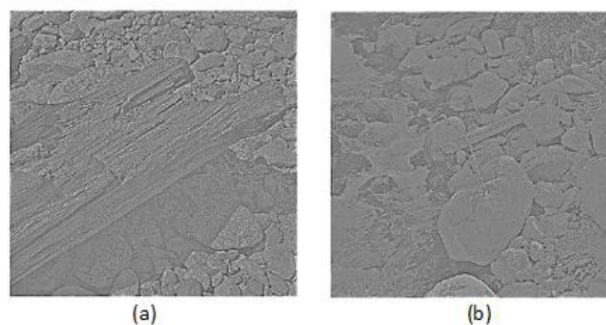


Fig 3. (a) Image 1 (b) Image 2

Table 1. Table of Manual Adaptation of Angle of Steerable Basis to Images Shown in Figure 3

For Image 1(a)		For Image 2 (b)	
Angle	Kurtosis	Angle	Kurtosis
0	7.4155	0	10.5524
$\pi/16$	7.5632	$\pi/16$	10.2035
$\pi/8$	7.428	$\pi/8$	9.9449
$\pi/4$	7.4908	$\pi/4$	10.4353
$-\pi/16$	7.2773	$-\pi/16$	10.3057
$-\pi/8$	7.4684	$-\pi/8$	9.8996
$-\pi/4$	7.5879	$-\pi/4$	10.3384

Figure 4 shows the steerable basis with different angles. Next, we investigated how angles of steerable basis converge to an optimal value for which the maximum of kurtosis is achieved. For that, we assigned initial random angles to the steerable basis

and ask for the optimal choice of steerable angle using MAP approach as discussed in Section 2. The angle obtained after MAP are observed to converge to a fixed value as shown in Table 2. For instance, initial significantly different steerable angles of $\pi/8$, 0, $-\pi/16$ result in different kurtosis for image shown in image 1 (Figure 3(a)), however, after MAP the steerable basis angle has converged to the optimal $\pi/4$. Similarly, initial significantly different angles of $-\pi/16$, 0, $\pi/8$ has also resulted in different kurtosis for image shown in image 2 (Figure 3 (b)), however, after MAP the angle has converged to the optimal $\pi/4$ value for which the maximum of kurtosis occurs. Usually, variance of coefficients is considered to measure the sparseness. Kurtosis, being the measure of fourth order moment is expected to measure the sparseness with high sensitivity compared to the variance which is a second order moment. The justification came from the fact that higher order moments better describe the distribution of coefficients⁽¹⁶⁾. This convergence of steerable basis angles can be observed in Table 3.

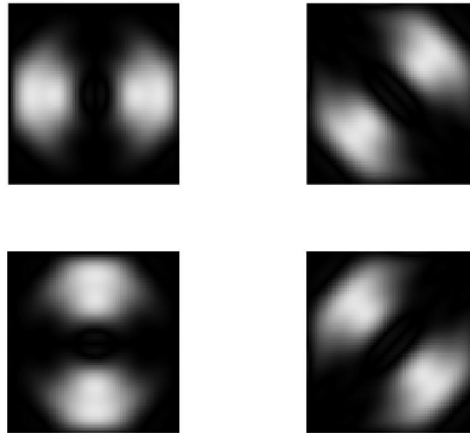


Fig 4. Steerable basis with considered angles values

Table 2. Table of Angle Adaptation After Learning of Steerable Basis Starting with Three Different Angles for Image 1 and Image 2

Image 1				Image 2			
Initial angle	steering	Kurtosis	Final angle after learning through MAP	Initial angle	steering	Kurtosis	Final angle after learning through MAP
$\pi/8$		7.3885	Nearer to $\pi/4$	$\pi/16$		10.4395	Nearer to $\pi/4$
0		7.331	Nearer to $\pi/4$	0		10.1499	Nearer to $\pi/4$
$-\pi/16$		7.5717	Nearer to $-\pi/4$	$-\pi/8$		10.2917	Nearer to $-\pi/4$

The results of angle learning using MAP for image 1 and image 2 is shown in Table 2. Hough transform, due to its capability to capture hidden geometries in natural images, has been extensively used in finding the features related to image compression. However, it requires manipulation of Hough transform for individual image separately which makes its usage limited. Though the manual cumbersome procedure of finding Hough transform, it is used for benchmarking of compression efficiency. Hence, we compare the MAP based learned angles of steerable basis with that of the angles derived from the Hough transform.

The learned angle for both the images are almost same as the angle chosen from Hough transform as shown in Table 3. Sparse coefficients obtained from the current proposals are compared with that of two existing mechanisms (Random basis and steered basis whose orientation is chosen from Hough transform).

Figures 5 and 6 show distribution of coefficients of said three techniques. The kurtosis of the distribution of coefficients is shown in Table 3.

We repeated same experiment for image 2 as shown in Figure 3(b).

As per inference from Hough transform discussed in section 1.3 the adaptation of angle of steerable basis for same image is $\pi/4$.

Table 3. Performance Comparison of Proposed Technique with Map Learning of Random Basis and Angle of Steerable Basis Inferred from the Hough Transform

	Kurtosis	
	Image 1	Image 2
From MAP learning of random basis	6.6502	8.5664
Angle of steerable basis inferred from the Hough transform	7.4155	10.3524
From the proposed MAP learning of angle of steerable basis	7.4908	10.4395

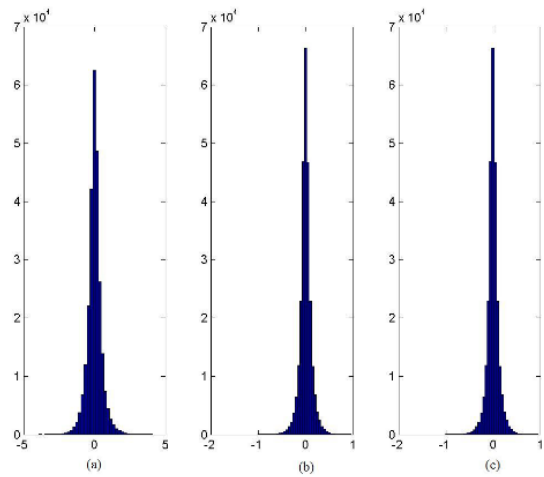


Fig 5. Histograms of coefficients of image 1 (a) real random basis (b) steerable basis angle selected using Hough Transform (c) steerable basis angle learned steerable basis

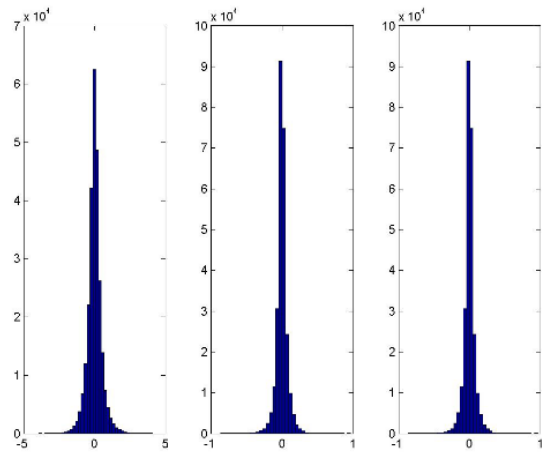


Fig 6. Histograms of coefficients of image 1 (a) real random basis (b) steerable basis angle selected using Hough Transform (c) steerable basis angle learned steerable basis

Discussion:

Sparse representation allows for higher compression ratios while maintaining acceptable image quality. Natural scenes often contain redundant information, where similar patterns or textures repeat across the images. Edges are fundamental features in natural images and often convey important information about object boundaries and structures. In addition, natural images typically include large smooth regions, such as skies, walls, or surfaces. These smooth regions can be represented efficiently using sparse coding techniques by capturing their low-frequency content with only a few coefficients. Sparse representation techniques capture edge information with sparse coefficients, allowing for efficient encoding and reconstruction.

Machine learning-based compression methods are based on the learning of features directly from the data. Rather than relying on predefined transformations such as DCT and wavelet Transforms, these methods train models to extract relevant features and represent the data in a compressed form. However, these methods may fail to perform better for the unseen data. In addition, the performance is dependent on the computational efficiency and effective training. On the other side, fixed Transform-based methods are often computationally efficient and have well-understood mathematical properties, making them suitable for real-time applications and standardization.

One approach to achieving a sparse transformation is through the training of a random basis of transformation using MAP learning. Initially, these random basis are trained in order to attain a sparse distribution of coefficients within the structure of WPS. Subsequently, following an adequate period of learning, it is observed that the random basis closely resembles steerable basis. Therefore, drawing inspiration from the upper technique in the proposed method, the authors meticulously addressed the orientation of the steerable basis. Here, the authors drew insights from the Hough transformation to properly align the steerable basis, resulting in a sparse transformation. The proposed approach involves the acquisition of angle knowledge pertaining to the steerable basis of the Wavelet Pyramid Structure (WPS), ultimately yielding optimal outcomes in relation to sparse transformation. This method eliminates the need for extensive learning periods, a notable contrast to the initial approach which necessitated the acquisition of random basis. Furthermore, the integration of steerable basis within the WPS framework ensures a reliable reconstruction of the input signal. A key advantage is the absence of manual Hough Transformation computations for the adjustment or calibration of steerable basis in sparse transformation processes. The comparative analysis presented in Tables 2 and 3 demonstrates the superior performance of the proposed method in contrast to other state of the art techniques. This is attributed to the exclusive emphasis on angle acquisition of steerable basis within the WPS, in contrast to random basis, thereby establishing a fixed structure. Moreover, the absence of human error is notable due to the elimination of manual Hough Transformation computations. Learning of angle of steerable basis does not depend on initial value as discussed in Section 3 and guarantees optimum angle for sparse transformation.

4 Conclusion

In this study, we introduce a methodology for angle learning of a steerable basis to attain a sparse representation of a given image. We adopt a learning approach like a previous technique, but rather than commencing with a set of randomly generated real basis, we initiate the learning process with a set of steerable basis. Upon learning the angles of the steerable basis, we observe that the acquired angles closely align with those obtained from the previous technique, indicating successful angle tuning of the steerable basis. This tuning process is facilitated by leveraging information from the Hough transform. In addition, our approach resulted in better compression efficiency with an improvement of almost 10 percent. This study can be extended further in future for the statistical analysis of the improvement observed across different genre of the images such as medical domain.

References

- 1) Johansson H. Sampling and quantization. In: Signal Processing and Machine Learning Theory. Academic Press. 2024;p. 185–265. Available from: <https://doi.org/10.1016/B978-0-32-391772-8.00011-9>.
- 2) Geng C, Huang S, Chen S. Recent advances in open set recognition: A survey. *IEEE Transactions on Pattern Analysis and Machine Intelligence*. 2020;43(10):3614–3631. Available from: <https://doi.org/10.1109/TPAMI.2020.2981604>.
- 3) Li J, Cui W, Zhang X. Projected Gradient Descent for Spectral Compressed Sensing via Symmetric Hankel Factorization. *IEEE Transactions on Signal Processing*. 2024;72:1590–1606. Available from: <https://doi.org/10.1109/TSP.2024.3378004>.
- 4) Zhou S, Deng X, Li C, Liu Y, Jiang H. Recognition-Oriented Image Compressive Sensing with Deep Learning. *IEEE Transactions on Multimedia*. 2022;25:2022–2032. Available from: <https://doi.org/10.1109/TMM.2022.3142952>.
- 5) Upadhyaya V, Salim M. Compressive Sensing: Methods, Techniques, and Applications. In: International Conference on Applied Scientific Computational Intelligence using Data Science (ASCI 2020);vol. 1099 of IOP Conference Series: Materials Science and Engineering. 2021;p. 1–23. Available from: <https://iopscience.iop.org/article/10.1088/1757-899X/1099/1/012012>.
- 6) Zhang Y, Wang Z, Zhang X, Cui Z, Zhang B, Cui J, et al. Application of improved virtual sample and sparse representation in face recognition. *CAAI Transactions on Intelligence Technology*. 2023;8(4):1391–1402. Available from: <https://doi.org/10.1049/cit.2.12115>.

- 7) Bian S, He X, Xu Z, Zhang L. Image Denoising by Deep Convolution Based on Sparse Representation. *Computers* . 2023;12(6):1–16. Available from: <https://doi.org/10.3390/computers12060112>.
- 8) Li X, Wan W, Zhou F, Jie Y, Tan H. Medical image fusion based on sparse representation and neighbor energy activity. *Biomedical Signal Processing and Control*. 2023;80(Part 2). Available from: <https://doi.org/10.1016/j.bspc.2022.104353>.
- 9) Olshausen BA, Field DJ. Emergence of simple-cell receptive field properties by learning a sparse code for natural images. *Nature*. 1996;381(6583):607–609. Available from: <https://doi.org/10.1038/381607a0>.
- 10) Zhou J, Zhang W, Li Y, Wang X, Zhang L, Li H. Phase-based displacement sensor with improved spatial frequency estimation and data fusion strategy. *IEEE Sensors Journal*. 2022;22(4):3306–3315. Available from: <https://doi.org/10.1109/JSEN.2022.3141110>.
- 11) Jiang W, Wang W, Chen Y. Neural Image Compression Using Masked Sparse Visual Representation. In: Proceedings of the IEEE/CVF Winter Conference on Applications of Computer Vision. 2024;p. 4177–4185. Available from: <https://doi.ieeecomputersociety.org/10.1109/WACV57701.2024.00414>.
- 12) Wang C, Wang Y, Deng D, Cao J, Zhao W. Multi-scale pyramidal hash learning for traditional building facade image retrieval. *International Journal of Machine Learning and Cybernetics*. 2024;15:2695–2707. Available from: <https://doi.org/10.1007/s13042-023-02057-4>.
- 13) Nguyen TS, Luong M, Kaaniche M, Ngo LH, Beghdadi A. A novel multi-branch wavelet neural network for sparse representation-based object classification. *Pattern Recognition*. 2023;135. Available from: <https://doi.org/10.1016/j.patcog.2022.109155>.
- 14) Ma W, Wang K, Li J, Yang SX, Li J, Song L, et al. Infrared and Visible Image Fusion Technology and Application: A Review. *Sensors*. 2023;23(2):1–23. Available from: <https://doi.org/10.3390/s23020599>.
- 15) Zhao T, Blu T. The Fourier-Argand representation: An optimal basis of steerable patterns. *IEEE Transactions on Image Processing*. 2020;29:6357–6371. Available from: <https://doi.org/10.1109/TIP.2020.2990483>.
- 16) Kravets V, Stern A. Progressive compressive sensing of large images with multiscale deep learning reconstruction. *Scientific Reports*. 2022;12:1–10. Available from: <https://doi.org/10.1038/s41598-022-11401-7>.